

# Dielectric Spectroscopy of an Anti-Ferroelectric Liquid Crystalline Material with Para- and Ferro-Electric Phases

**Avneesh Mishra, Abhay S. Pandey and R. Dhar**

Soft Materials Research Laboratory  
Centre of Materials Sciences, Institute of Interdisciplinary Studies  
University of Allahabad, Allahabad  
Email: [dr\\_ravindra\\_dhar@hotmail.com](mailto:dr_ravindra_dhar@hotmail.com)

**R. Dabrowski**

Institute of Applied Sciences and Chemistry  
Military University of Technology, Warsaw (Poland)

(Received January 12, 2014)

**Abstract:** The dielectric studies have been carried out in the frequency range of 1 Hz to 35 MHz under planar anchoring conditions of the studied material (S)-(+)-4-(1-ethylheptyloxycarbonyl) phenyl 4'-(6-perfluorooctanoyloxy hex-1-oxy) biphenyl-4-carboxylate exhibiting paraelectric  $SmA^*$ , ferroelectric  $SmC^*$  and a wide temperature range ( $\sim 83^\circ\text{C}$ ) anti-ferroelectric  $SmC_a^*$  phases. The soft mode relaxation due to tilt-fluctuation of molecules is observed in MHz region for the  $SmA^*$  phase. The relaxation frequencies decreases and dielectric strength increases ( $\sim 0.2\text{--}3.4$ ) with decrease in the temperature for observed soft mode relaxation and follows Curie–Weiss law. The  $SmC^*$  phase shows Goldstone mode relaxation due to phase fluctuation of molecules with relaxation frequency  $\sim 10$  kHz. Only one mode of relaxation has been observed in the  $SmC_a^*$  phase presumably due to anti-ferroelectric ordering of the molecules. Its dielectric strength varies from  $\sim 0.55$  at  $104.3^\circ\text{C}$  to  $2.20$  at  $37.6^\circ\text{C}$ .

**Keywords:** Anti-ferroelectric, liquid crystalline material, dielectric spectroscopy, tilts and phase fluctuation modes.

## 1. Introduction

Materials in which molecules are oriented similar to that of ferroelectric liquid crystals (FLCs) in each smectic layers but the direction of tilt may alternate to form a herringbone structure are called smectic  $C_a^*$  or anti-ferroelectric liquid crystal (AFLC). Chandani *et. al.*<sup>1</sup> reported anti-ferroelectricity in liquid crystals. The FLC and AFLC materials have attracted much attention of researchers due to their technological

applications as well as fundamental study of molecular structure and properties<sup>2-4</sup>. Orthoconic AFLCs are specifically important from application point of view because of low layer shrinkage at  $SmA^* - SmC^*$  transition<sup>5, 6</sup>. Anti-ferroelectric liquid crystals (AFLCs) possess excellent electro-optical properties like tri-state switching behavior, easy DC compensation, microsecond response, gray scale capability, wide viewing angle besides the memory property and large hysteresis. The first AFLC material was synthesized by Levelut *et. al.*<sup>7</sup> in 1983.

In this communication, we report the dielectric spectroscopy of a room temperature AFLC material namely (S)-(+)-4-(1-ethylheptyloxycarbonyl) phenyl 4'-(6-perfluorooctanoyloxy hex-1-oxy) biphenyl-4-carboxylate, abbreviated as (S) 7F6Bi<sup>8</sup>. The chemical structure of 7F6Bi is as follows:

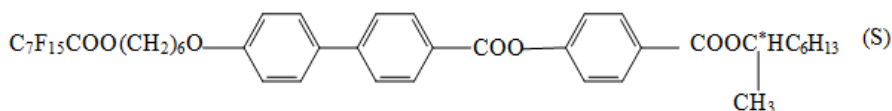


Figure 1: Molecular structure of (S)-(+)-4-(1ethylheptyloxycarbonyl) phenyl 4'-(6-perfluorooctanoyloxyhex-1-oxy) biphenyl-4-carboxylate ((S) 7F6Bi).

## 2. Experimental Techniques

Thermodynamic studies have been carried out with the help of Differential Scanning Calorimeter (DSC) of NETZSCH (model DSC 200 F3 Maia). The dielectric measurements have been carried out with a gold coated planar dielectric cell of 36.5 pF active capacitance ( $C_L$ ) from AWAT, Warsaw, Poland, whose glass plates are separated by a spacer of thickness 8.8  $\mu\text{m}$ . Dielectric data have been acquired with the help of Newton's Phase Sensitive Multimeter (model-1735) coupled with Impedance Analysis Interface (model-1257) in the frequency range of 1 Hz to 35 MHz. The temperature of the sample has been controlled with the help of a hot stage (Instec model HCS 302) joined with temperature controller (Instec-model mK 1000). The measured dielectric spectrum can be described with the help of generalized Cole-Cole<sup>9, 10</sup> equation:

$$(1) \quad \varepsilon^* = \varepsilon' - j\varepsilon'' = \varepsilon(\infty) + \sum_i \frac{(\Delta\varepsilon)_i}{1 + (j\omega\tau_i)^{1-h_i}} + \frac{A}{\omega^n} - j \frac{\sigma_{ion}}{\varepsilon_0\omega^k} - jBf^m$$

where  $(\Delta\varepsilon)_i$ ,  $\tau_i$  and  $h_i$  are the dielectric strength, the relaxation time and the symmetric distribution parameter  $0 \leq h_i \leq 1$  of the  $i^{th}$  mode, respectively,

$\epsilon(\infty)$  is high frequency limiting values of the permittivity; the third and fourth terms in equation (1), represent the contribution of the electrode polarization capacitance and ionic conductance at low frequencies where A and n are constants<sup>11</sup>. The fifth imaginary term  $Bf^m$  is included in equation (1) to partially account for the high-frequency electrode surface resistance<sup>12, 13</sup>, B and m being constants.

### 3. Results and Discussion

Results obtained and relevant discussions have been given in the following sub sections.

#### 3.1 Thermodynamic studies

DSC traces in the cooling cycles of the studied material (7F6Bi) at the scanning rate of 2.5 °C/min is shown in Figure 2.

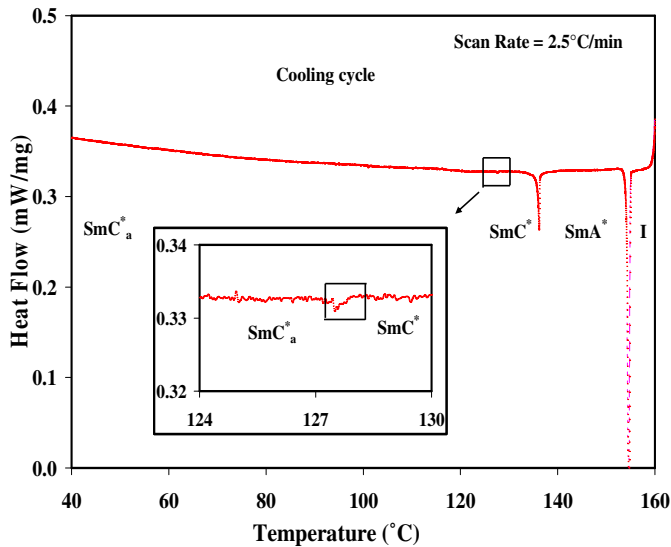


Figure 2: DSC thermogram of 7F6Bi in cooling cycle at 2.5 scanning rate. The peaks are representing to the transition temperatures. Inset shows expanded view of the  $SmC_a^*$  phase transition peaks.

According to the DSC results, following phase sequences have been observed in cooling cycle:

$$I (154.7^\circ\text{C}) \rightarrow SmA^* (136.1^\circ\text{C}) \rightarrow SmC^* (127.8^\circ\text{C}) \rightarrow SmC_a^*$$

The  $SmC^*$  to  $SmC_a^*$  phase transition peak is weak and it could not be observed due to smearing of the transition peaks at high and low scanning

rates. But proper magnification of the cooling thermogram, it could be possible to detect the  $SmC^*$  to  $SmC_a^*$  transition peak at the scan rate of 2.5 °C/min.

### 3.2 Dielectric spectroscopy

The highest value of permittivity ( $\epsilon'_\perp$ ) has been observed  $\sim 106$  in the  $SmC^*$  phase at 100 Hz. Below 100 Hz the value of  $\epsilon'_\perp$  increases with decrease in frequency due to the contribution of electrode polarization capacitance and ionic conductance at all temperatures<sup>11</sup>. The large variation in  $\epsilon'_\perp$  with frequency has been appeared in the  $SmA^*$  and  $SmC^*$  due to the dielectric relaxation modes present in these phases. On further cooling in the  $SmC_a^*$  phase, the material has crystallized near the room temperature ( $\sim 43^\circ\text{C}$ ). The characteristics parameters of all observed modes in different phases have been obtained by fitting to the experimental data with theoretical equation (1). The results obtained from the fitting are shown in Figure 3.

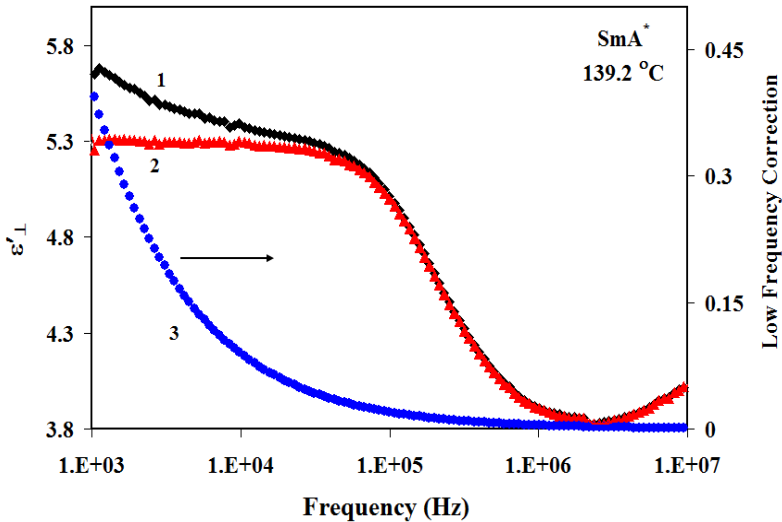


Figure 3: Variation of the real part ( $\epsilon'_\perp$ ) of the permittivity with frequency. Curve 1 (rhombus) shows the experimental data, curve 2 (solid line) shows the best-fit of the experimental data, curve 3 (square) shows the low frequency correction term (read on right vertical scale) and curve 4 (triangle) represent the soft mode after subtracting the low frequency correction terms from the experimental data).

Figure 4 shows the temperature dependence of the relaxation frequencies of various modes observed in  $SmA^*$ ,  $SmC^*$  and  $SmC_a^*$  phases respectively.

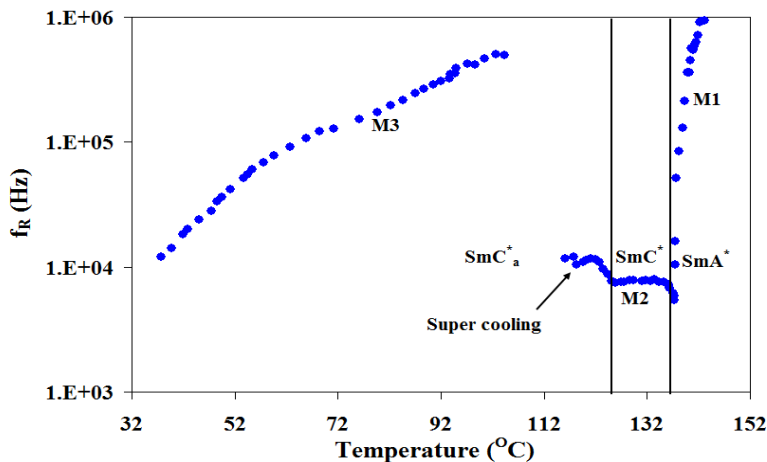


Figure 4: Temperature dependence of relaxation frequencies ( $f_R$ ) of various relaxation modes observed in different mesophases. Vertical lines show the transition temperature on the basis of thermodynamic study.

In the  $SmA^*$  phase, one dielectric relaxation mode (M1) appears at  $\sim 143^\circ\text{C}$  with its relaxation frequency at 938 kHz. Its dielectric strength is found to be small  $\sim (0.2 \text{ to } 3)$ . On the basis of the molecular structure of  $SmA^*$  phase and its temperature dependence behavior, mode M1 have to correspond to a soft mode which is associated with director tilt fluctuation of the molecules in the smectic layers<sup>14</sup>. Due to high relaxation frequency and weak dielectric strength M1 could not be detected above  $143.2^\circ\text{C}$ . The dielectric strength of the soft mode follows the Curie-Weiss law  $\Delta\epsilon' = C/(T - T_c)$ , where  $C$  is a curie constant and  $T_c$  is the Curie temperature of transition from  $SmA^*$  to  $SmC^*$  phase. From Curie-Weiss law,  $T_c$  has been found to be  $137.4^\circ\text{C}$  for  $SmA^*$  to  $SmC^*$  transition which agrees with the other dielectric parameter.

Dielectric relaxation mode M2 has been appeared in  $SmC^*$  phase. Throughout  $SmC^*$  phase,  $f_R$  remains almost constant ( $\sim 5.6 \text{ to } 7.6 \text{ kHz}$ ) whereas  $\Delta\epsilon'$  increases (7.69 to 14.63). The distribution parameter of mode M2 has been found to be greater than soft mode of  $SmA^*$  phase; which appears due to the tilted structure of phase. M2 has been attributed to the Goldstone mode (GM) arising due to the precession of the tilted molecules

around the helicoidal axis<sup>15</sup>. GM seems to penetrate into the  $SmC_a^*$  phase (see Figure 4).

In the  $SmC_a^*$  phase, only one relaxation mode M3 has been observed. Hiraoka *et. al.*<sup>16</sup> also have reported only one relaxation mode at  $\sim 1$  MHz in the  $SmC_a^*$  phase. In present studies, the observed mode seems due to anti-phase fluctuations of the azimuthal angle i.e. so called anti-ferroelectric Goldstone mode. The mode due to in-phase fluctuations of the azimuthal angle is not detected here in our studies. The dielectric strength of M3 varies from 0.5 to 2.2. The Cole-Cole plot of  $SmC_a^*$  phase is shown in Figure 5.

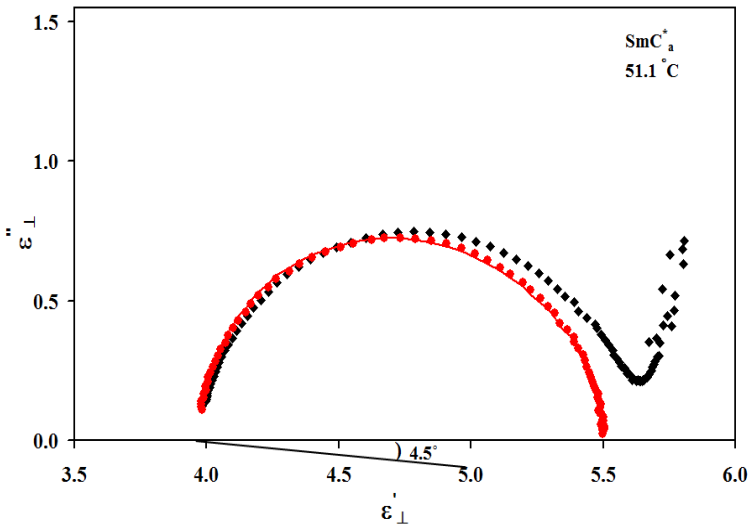


Figure 5: Cole-Cole arcs of  $SmC_a^*$  phase at 51.1°C. The experimental data and corrected data (experimental data – correction terms) are shown by rhombus and circle respectively. The solid line shows the best fitting of the experimental data. Values of the distribution parameter are mentioned in degree.

## 4. Conclusions

The following results have summarized:

- From the dielectric study, it has been observed that the AFLC material (S-7F6Bi) goes into broad temperature range anti-ferroelectric  $SmC_a^*$  with two other different liquid crystalline phases as para-electric  $SmA^*$  and ferroelectric  $SmC^*$ .
- Soft mode has been observed in the  $SmA^*$  phase and Goldstone mode has been observed in  $SmC^*$  phase. In  $SmC_a^*$  phase only one mode

has been observed due to the anti-phase fluctuation in the azimuthal angle.

### Acknowledgments

We thank DAE-BRNS for financial assistance under a research grant No. 2010/34/38/BRNS.

### References

1. A. D. L. Chandani, Y. Ouchi, H. Takezoe, A. Fukuda, K. Terashima, K. Furukawa and A. Kishi, Novel Phases Exhibiting Tristable Switching, *Jpn. J. Appl. Phys. Part 2*, **28(7)** (1989) L1261–L1264.
2. N. A. Clark and S. T. Lagerwall, Submicrosecond bistable electro-optic switching in liquid crystals, *Appl. Phys. Lett.*, **36** (1980) 899–901.
3. A. D. L. Chandani, T. Hagiwara, Y. Suzuki, Y. Ouchi, H. Takezoe and A. Fukuda, *Jpn. J. Appl. Phys. Part 2*, **27(5)** (1988) L729–L732.
4. M. Johno, K. Itoh, J. Lee, Y. Ouchi, H. Takejoe, A. Fukuda and T. Kitazume, Temporal and Spatial Behavior of the Field-Induced Transition between Antiferroelectric and Ferroelectric Phases in Chiral Smectics, *Jpn. J. Appl. Phys.*, **29** (1990) L107–L110.
5. J. P. F. Lagerwall, A. Saipa, F. Giesselmann and R. Dabrowski, On the origin of high optical director tilt in a partially fluorinated orthoconic antiferroelectric liquid crystal mixture, *Liq. Cryst.*, **31(9)** (2004) 1175–1184.
6. J.P. F. Lagerwall and F. Giesselmann, Current Topics in Smectic Liquid Crystal Research, *Chem. Phys. Chem.*, **7(1)** (2006) 20–45.
7. A. M. Levelut, C. Gemain, P. Keller, L. Liebert and J. Billard, Two new mesophases in a chiral compound, *J. de Physique*, **44(5)** (1983) 623–629.
8. J. Gasowska, R. Dabrowski, W. Drzewinski, M. Filipowicz, J. Przedmojski and K. Kenig, Comparison of Mesomorphic Properties in Chiral and Achiral Homologous Series of High Tilted Ferroelectrics and Antiferroelectrics, *Ferroelectrics*, **309(1)** (2004) 83–93.
9. K. S. Cole and R. H. Cole, Dispersion and Absorption in Dielectrics I. Alternating Current Characteristics, *J. Chem. Phys.*, **9(4)** (1941) 341–351.
10. M. Gupta, R. Dhar, V. K. Agrawal, R. Dabrowski and M. Tykarska, Dielectric spectroscopy of a binary mixture of liquid crystals showing wide temperature range twisted grain boundary phase with re-entrant cholesteric phase, *Phys. Rev. E*, **72(2)** (2005) 021703(1–10).
11. S. L. Srivastava and R. Dhar, Characteristic time of ionic conductance and electrode polarization capacitance in some organic liquids by low frequency dielectric spectroscopy, *Indian J. Pure Appl. Phys.*, **29(11)** (1991) 745–751.
12. S. L. Srivastava, A High Frequency Impedance Model, *Proc. Natl. Acad. Sci. India*, **63** (1993) 311–332.

13. R. Dhar, An impedance model to improve the higher frequency limit of electrical measurements on the capacitor cell made from electrodes of finite resistances, *Indian J. Pure Appl. Phys.*, **42** (2004) 56–61.
14. M. Buivydas, F. Gouda, G. Andersson, S. T. Lagerwall, B. Stebler, J. Bomelburg, G. Heppke and B. Gestblom, Collective and non-collective excitations in antiferroelectric and ferroelectric liquid crystals studied by dielectric relaxation spectroscopy and electro-optic measurements, *Liq. Cryst.*, **23**(5) (1997) 723–739.
15. A. Levstik, T. Carlsson, C. Filipic, I. Levstik and B. Zeks, Goldstone mode and soft mode at the smectic-A–smectic-C<sup>/emph></sup> phase transition studied by dielectric relaxation, *Phys. Rev. A*, **35**(8) (1987) 3527–3584.
16. K. Hiraoka, A. Taguchi, Y. Ouchi, H. Takezoe and A. Fukuda, Observation of three subphases in smectic C\* of MHPOBC by dielectric measurements, *Jpn. J. Appl. Phys.*, part 2, **29**(1) (1990) L103–L106.